PPPL--2511

DE88 009346

Profile Correction to Electron Temperature and Enhancement Factor in Soft X-ray Pulse-Height-Analysis Measurements in Tokamaks

S. SESNIC, M. DIESSO, K. HILL, A. HOLLAND
Princeton University, Plasma Physics Laboratory, P.O.Box 451, Princeton, N.J. 08543
and F. POHL
Max-Planck Institut für Plasmaphysik, 8046-Garching, F.R. Germany

Abstract

Because soft x-ray pulse-height-analysis (PHA) spectra contain chordal information, the electron temperature and the radiation intensity (enhancement factor) measurements do not represent the local values. Assuming that the profile Ansatz for the electron temperature and density is of the form $n_{eo}[1-(r/a)^2]^{\alpha}$ and $kT_{eo}[1-(r/a)^2]^{\beta}$, we obtain the correction factors for the electron temperature and the enhancement factor as a function of the profile coefficients α and β and the energy at which the evaluation was made. The corrected values of the temperature is typically between 1 to 10 % higher than the values derived from the raw chordal spectra. We also correct the measured radiation intensity for the profile effects. Finally, the spectrum distortion due to pulse pile-up effects is evaluated. A set of curves is given from which the distortion of the spectrum can be obtained, if the electron temperature, the Be or Al filter thickness, and the electronic parameters of the acquisition system are known.

INTRODUCTION

The pulse-height-analysis (PHA) system[1-3] measures the soft x-ray spectrum along the line of sight. Because this is the line of sight measurement, the measured spectrum is an overlay of spectra coming from regions of different electron temperatures and densities and, therefore, the slope of the measured spectrum representing the electron temperature does not exhibit a unique value. Since the measured temperature is not a correct peak temperature, it is of interest to know how to estimate the error in measurement or even how to correct this value. This error depends very strongly on the electron temperature and density profiles and it is important to find the functional dependence of the correction factor on the profile parameters. These profile parameters can vary in today's tokamaks very much, because they depend on the heating

method (neutral beam heating, ICRH, ECH, etc.) and on the fuelling method (gas, pellets, neutral beam). Both heating and fuelling can be carried out either in the center or at the edge of the plasma, resulting in large differences in the temperature and density profiles.

One way of finding the correct temperatures is to make a set of measurements along different lines of sight and then to make an Abel inversion.[4] In the case where one has only one or only a few line of sight measurements, one cannot make the Abel inversion. In this case one has to find other ways to correct the measured values. In this paper we are concerned with this other case, where there are only a few lines of sight measurements. To obtain the correct values for the electron temperature from a single line of sight measurement one has either to know the form of the electron temperature and density profiles or at least know these forms approximately. Our method is based on such an assumption that we know these profiles at least to a certain degree. The profile forms, for example, could be obtained from laser scattering. In this case, since the correct temperature is presumably found from the laser scattering experiment, the temperature correction per se would not be so important. However, the PHA measurement also allows one to find the radiation enhancement coefficient ζ from which one can deduce the local Z_{eff} values[1-4] at each line of sight position. (The enhancement coefficient ζ is defined as a ratio of the measured continuum to a pure hydrogen bremsstrahlung. It is normally always larger than 1 due to the presence of impurities in the real plasma, which cause, on one hand, an increase in bremsstrahlung radiation and, on the other hand, an appearance of a strong recombination radiation.) The accuracy of the ζ or Z_{eff} values depends on the accuracy of the electron temperature value. Therefore, even if we know the electron temperature from some other measurement, we still need to correct the PHA electron temperature and the enhancement coefficient in order to obtain the corrected local Z_{eff} and corrected local impurity densities obtained from the PHA line radiation and ζ measurements.

Another distortion of the spectra is caused by pulse pile-up effects. If two or more photons arrive within a time period shorter than the time needed for the electronics to recognize a single pulse, the electronics system will register these two or more photons as a single photon of the energy nearly equal to the sum of energies of the single photons. This distorts both the electron temperature and enhancement coefficient measurement. Various aspects of this problem have been handled by differen: authors.[5-7] This paper presents only the corrections to the enhancement coefficient as a function of the electron temperature and the filter material and thickness, although the distortion of the electron temperature is also implied in the discussion.

In part I we discuss the corrections to the electron temperature and enhancement coefficient for various profiles and photon energies. In part II we discuss the corrections to the enhancement coefficient for different filter thicknesses and electron temperatures.

I. ELECTRON TEMPERATURE AND ENHANCEMENT COEFFICIENT CORRECTION

In the case of a pure continuum radiation without line radiation, setting the Gaunt factor equal to 1 and with the density, electron temperature, and enhancement coefficient profiles represented as $n_e(z)$, $kT_e(z)$, and $\zeta(z)$ the measured radiation spectrum can be described by the theoretical expression[1]

$$S(p,E) = 2\ A \int^{L} \zeta(z)\, n_e^2(z) \exp\left[-E / kT_e(z)\right] / \left[kT_e^{1/2}(z)\right] dz, \qquad (1)$$

where A is the radiation constant, E is the photon energy, and z is the position along the line of sight, L. For the purpose of demonstrating this correction method we assume a circular plasma and approximate the plasma profiles by $n_e(\rho) = n_{eo}(1-\rho^2)^{\alpha}$, $kT_e = kT_{eo}(1-\rho^2)^{\beta}$ and, for simplicity, assume $\zeta(\rho) = \zeta_o$. Here we introduce $\rho = r/a$, where r is the minor radius and a is the plasma size. We also introduce the normalized tangency radius $p = r_t/a$, with r_t being the minimum distance between the line of sight and the center of the plasma. In general, we are interested in the off-axis measurements of $kT_e(p)$ and not kT_{eo} (they, of course, coincide if $p = 0$). Therefore, $kT_e(\rho) = kT_e(p)[(1-\rho^2)/(1-p^2)]^{\beta}$ and $n_e(\rho) = n_e(p)[(1-\rho^2)/(1-p^2)]^{\alpha}$ should describe well the profiles in the vicinity of $\rho = p$.

The measured spectrum, which should be equal to the theoretical spectrum in expression (1), can be approximated by

$$S_m(E) = \exp\left(a / E + b + c\, E + d\, E^2\right), \qquad (2)$$

where a, b, c, and d are constants obtained by fitting the measured spectrum. If we simplify the fitting and set $a = d = 0$ and retain b and c only, the following arguments and the correction formulas still apply. The (incorrect) measured temperature T_m can be obtained from the fitted measured spectrum simply by finding the negative inverse of the slope of the natural logarithm of S_m at the energy E

$$T_m(E) = -1/(d \ln S_m/dE) = -1/(-a/E^2 + c + 2d\, E). \qquad (3)$$

This electron temperature is not the correct temperature. We would , therefore, like to find the correction factor T_c/T_m, where $T_c = kT_e(p)$ is the correct value of the temperature at the tangency radius p. Note also that this measured temperature depends on the energy at which it was evaluated from the slope of the measured spectrum. For the purpose of finding the correct temperature in a more general form we define the normalized effective plasma thickness at $\rho = p$:

$$I(p) = \langle L \rangle /2a = S(p) / \{A\, \zeta(p)\, n_e^2(p) \exp[-E / kT_e(p)] / [kT_e^{1/2}(p)]\}. \qquad (4)$$

The effective thickness is the thickness of an equivalent homogeneous plasma of temperature $kT_e(p)$ and density $n_e(p)$ (plasma values at tangency radius) such that its radiation intensity at energy E is equal to that of the measured spectrum at the same energy E. It is obvious from the expression (4) that the effective thickness $\langle L \rangle$ is not a constant but that it varies with energy.

By taking the natural logarithm of I(p) and defining it as $\Lambda = \ln I(p)$, by normalizing energy in terms of the incorrect electron temperature T_m, $\varepsilon = E/T_m$, and by utilizing expressions (1), (2), and (3) in (4), we obtain for the correction factor

$$T_c/T_m = (1 + d\Lambda/d\varepsilon)^{-1}. \qquad (5)$$

To determine the ratio of the corrected enhancement coefficient ζ_c to the measured coefficient ζ_m one also must have the correct and measured values of the spectrum intercepts S_{oc} and S_{om}. The intercept is defined as the value of the spectrum S at E = 0. Since the intercept value is $S_o = S(E) \exp(E/kT_e)$, where S(E) is the value of the either correct or measured spectrum at the energy E, one can show that $S_{oc}/S_{om} = \exp(\varepsilon\, d\Lambda/d\varepsilon)$. The measured and corrected values of the enhancement coefficient in terms of the corresponding intercept values are given by $\zeta_m = S_{om} T_m^{1/2}/[A\, 2a\, (1 - p^2)^{1/2}\, n_e^2(p)]$ and $\zeta_c = S_{oc} T_c^{1/2}/[A \langle L \rangle\, n_e^2(p)]$, where A is again the appropriate radiation constant. Note that the measured enhancement coefficient ζ_m is obtained by averaging the radiation intensity over the pertinent line of sight length $2a(1 - p^2)^{1/2}$.

The correction factor for the enhancement coefficient now becomes

$$\zeta_c/\zeta_m = \exp(\varepsilon\, d\Lambda/d\varepsilon)\,(1 - p^2)^{1/2} / [1\ (1 + d\Lambda/d\varepsilon)^{1/2}]. \qquad (6)$$

The expressions (4), (5), and (6) are valid for any type of plasma form and profile, not only for the circular plasma assumed above. The expressions (5) and (6) were numerically evaluated for the profiles with α and β parameters and the results are shown in Figs. 1 to 10 for normalized energies ε = 1.0, 2.5, 5.0, 7.5, and 10.0. The error in electron temperature, incurred by taking simply the slope of the measured spectrum for the electron temperature, can be very large for small normalized energy: as high as 70% for the profiles with lowest α's and highest β's. With the increase of normalized energy this error becomes smaller and smaller, e.g., at ε = 10 and β = 2 the error in electron temperature decreases to less than 5% (T_c/T_m = 1.05). The error in temperature increases also with β, i.e., with a more peaked temperature profile. On the other hand, the error in temperature increases with decreased α, i.e., with a broader density profile.

The error in ζ estimates, i.e., the correction factor ζ_c/ζ_m, increases with both α and β (profile peakedness). The ζ_c/ζ_m values are normally high because of the definition of ζ_m — the measured radiation is averaged over the full length of the radiation path, in this case over 2a.

The dependence of the error (correction factor) on the normalized energy, i.e., on the energy in the spectrum, where the measurement is done, is shown in Figs. 11 to 16. The higher the normalized energy (the further in the spectrum we take the measurement), the smaller the error in electron temperature, which is something we expected. At the same time the error in the ζ estimate is larger. The error in both kT_e and ζ estimates increases with β (electron temperature peakedness), which is, of course, the same dependence as seen in Figs. 1 to 10. The error in kT_e, however, slightly decreases with α. The error in ζ with increasing α changes even less, but instead of decreasing, it increases.

The errors in estimating the electron temperature and enhancement coefficient depend on the position of the line of sight, p. This is shown in Figs. 17 and 18, where the correction factors T_c/T_m are presented as a function of p and β, but where α and ε are kept constant. The electron temperature correction factor T_c / T_m is not a very strong function of p, but the enhancement coefficient correction factor ζ_c / ζ_m increases very much for p's close to 1, i.e., near the edge of the plasma. This enhancement coefficient correction factor increases also very strongly with the increasing peakedness (β) or temperature gradient at the edge of the plasma .

II. PULSE PILE-UP CORRECTION

A PHA system usually has two electronic circuits to process the single pulses: a fast one and a slow one. The fast circuit recognizes and counts the single pulses. The minimum time interval between two pulses for the fast system to recognize them as single pulses is τ. The slow electronic circuit processes the single pulses and the processing time τ_s is much longer than τ. The pulses arriving within a time interval longer than τ_s are processed. Those pulses that arrive within a time interval shorter than τ_s but longer than τ are recognized as double pulses, which would, if processed, distort the spectrum, and are, therefore, rejected. The pulses coming within the time interval shorter than τ are not recognized as double, triple, etc. pulses, but as a single pulse equal in energy to their sum. They, therefore,will be processed and will distort the measured spectrum. The purpose of this part of the paper is to find the distortion of the spectrum due to double pulses and to the presence of an x-ray filter. The triple and higher order pulses[7] are not discussed in this paper.

A measured soft x-ray spectrum can be represented in terms of the normalized energy $\varepsilon = E / kT_e$, the transmission function of the x-ray filter $F(E) = \exp[-\mu(E)\, d]$, and the photon count rate N_c (photons per second) as

$$S(\varepsilon) = N_c \left\{ \int_0^\infty F(E)\ [\exp(-\varepsilon)/\varepsilon]\, d\varepsilon \right\}^{-1} F(E)\ \exp(-\varepsilon)/\varepsilon, \qquad (7)$$

where $\mu(E)$ is the total x-ray photon attenuation cross section of a given filter material and d is the thickness of the filter. The attenuation cross section can be mostly approximated by a function $\mu(E) = A\, E^{-B}$, where A and B are constants of the material with B having a value close to 3. Considering the coincidence of only two pulses during the time interval τ, it has been shown[5] that the double pulse spectrum can be described by the convolution integral

$$\tilde{S}(\varepsilon) = \tau / 4 \int_0^\infty S(\varepsilon')\, S(\varepsilon - \varepsilon')\, d\varepsilon'. \qquad (8)$$

We assume here that the pulses are of rectangular shape with a width of τ. A better approximation for the shape of the pulses would be to take a triangular pulse[6] of the same width τ.

Defining a normalized ratio of the double pulse spectrum to the original spectrum as $R_N = 4\,\tilde{S}(\varepsilon) / [\tau\, N_c\, S(\varepsilon)]$, we obtain for the normalized ratio

$$R_N(\varepsilon) = \varepsilon\, \exp\left[A\, d\, (\varepsilon\, kT_e)^{-B}\right] \left\{\int_0^\infty \exp\left[-A\, d\, (\varepsilon\, kT_e)^{-B}\right] \exp(-\varepsilon) / \varepsilon\, d\varepsilon\right\}^{-1} *$$

$$* \int_0^\infty \exp\left\{-A\, d\; kT_e^{-B}\left[(\varepsilon')^{-B} + (\varepsilon - \varepsilon')^{-B}\right]\right\}\left\{\varepsilon'(\varepsilon - \varepsilon')\right\}^{-1} d\varepsilon'. \qquad (9)$$

The parameters in this expression are the filter material constants A and B, the electron temperature kT_e, and the variable is the normalized energy ε. This expression has been numerically evaluated. The numerical results for the beryllium filter are shown in Figs. 19 to 21 and for the aluminum filter in Figs. 22 and 23. Since the expression (9) depends on several parameters and variables, we define a new parameter $D = A\, d\, (kT_e)^{-B}$, which characterizes the filter function not in terms of photon energy but in terms of electron temperature. The expression (9) then depends only on this new parameter D and on the normalized energy ε. Figures 19 and 22 then show the dependence of this parameter D for the given filter material on the electron temperature. In Figs. 20, 21, and 22 the normalized double spectrum ratio R_N is shown as a function of the normalized energy with D as a parameter.

The plots in Figs. 19 to 23 are used to find the spectral distortion for a measured spectrum at any energy ε. Knowing the electron temperature at least approximately and knowing the filter thickness, we find in Fig. 19 or 22 the value of the parameter D. With this value of D we go to Fig. 20, 21, or 23 and find the ratio R_N at any normalized energy ε. Knowing the pulse *pile-up constant τ of the electronic circuit and the measured count rate N_c, we can obtain the* relative spectral distortion $\tilde{S}(\varepsilon)/S(\varepsilon) = R_N\, \tau\, N_c / 4$, where again $S(\varepsilon)$ is the undistorted spectrum. From the value of the spectral distortion we can easily correct the value of the enhancement coefficient.

ACKNOWLEDGMENT

This work has been supported by U.S. DoE Contract No. DE-AC02-76-CHO-3073.

REFERENCES

[1]S. von Goeler, W. Stodiek, H. Eubank, H. Fishman, S. Grebenshchikov, and E.Hinnov, Nucl. Fusion **15**, 301 (1975).

[2]S. Sesnic, Max-Planck Institut für Plasmaphysik Report, IPP III/2, (1976).

[3]Equipe TFR, Nucl. Fusion **17**, 2 (1977).

[4]E. H. Silver, M. Bitter, K. Brau, D. Eames, A. Greenberger, K. W. Hill, D. M. Mead, W. Roney, N. R. Sauthoff, and S. von Goeler, Rev. Sci. Instrum. **53**, 1198 (1982).

[5]S. von Goeler, W. Stodiek, H. Eubank, Y. Sun, P. Thompson, and S. Slusky, Princeton Plasma Physics Laboratory Report No. MATT-1060, (1975).

[6]G. R. Dyer, G. H. Nielson, and G. G. Kelley, Nucl. Instrum. Methods **161**, 365 (1979).

[7]F. H. Tenney, Nucl. Instrum. Methods **219**, 165 (1984).

FIGURE CAPTIONS

FIG. 1. Electron temperature correction factor T_c/T_m as a function of the electron density and temperature profile parameters α and β and for the normalized energy $\varepsilon = 1$ and $p = 0$.

Fig. 2. Electron temperature correction factor T_c / T_m for $\varepsilon = 2.5$ and $p = 0$.

Fig. 3. Electron temperature correction factor T_c / T_m for $\varepsilon = 5$ and $p = 0$.

Fig. 4. Electron temperature correction factor T_c / T_m for $\varepsilon = 7.5$ and $p = 0$.

Fig. 5. Electron temperature correction factor T_c / T_m for $\varepsilon = 10$ and $p = 0$

Fig. 6. Enhancement coefficient correction factor ζ_c/ζ_m as a function of the electron density and temperature profile parameters α and β and for the normalized energy $\varepsilon = 1$ and $p = 0$.

Fig. 7. Enhancement coefficient correction factor ζ_c / ζ_m for $\varepsilon = 2.5$ and $p = 0$.

Fig. 8. Enhancement coefficient correction factor ζ_c / ζ_m for $\varepsilon = 5$ and $p = 0$.

Fig. 9. Enhancement coefficient correction factor ζ_c / ζ_m for $\varepsilon = 7.5$ and $p = 0$.

Fig. 10. Enhancement coefficient correction factor ζ_c / ζ_m for $\varepsilon = 10$ and $p = 0$.

Fig. 11. Electron temperature correction factor T_c / T_m as a function of the normalized energy ε and electron temperature profile parameter β and for $\alpha = 0.5$ and $p = 0$.

Fig. 12. Electron temperature correction factor T_c / T_m for $\alpha = 1$ and $p = 0$.

Fig. 13. Electron temperature correction factor T_c / T_m for $\alpha = 2$ and $p = 0$.

Fig. 14. Enhancement coefficient correction factor ζ_c/ζ_m as a function of the normalized energy ε and electron temperature profile parameter β and for $\alpha = 0.5$ and $p = 0$.

Fig. 15. Enhancement coefficient correction factor ζ_c / ζ_m for $\alpha = 1$ and $p = 0$.

Fig. 16. Enhancement coefficient correction factor ζ_c / ζ_m for $\alpha = 2$ and $p = 0$.

Fig. 17. Dependence of the electron temperature correction factor T_c / T_m on the sight line position p and electron temperature profile coefficient β but for constant α and ε.

Fig. 18. Dependence of the enhancement coefficient correction factor ζ_c / ζ_m on p and β with α and ε being constant.

Fig. 19. Filter parameter $D = A\, d\, kT_e^{-B}$ for beryllium foil as a function of the electron temperature kT_e and filter thickness d.

Fig. 20. Normalized double pulse spectrum R_N as a function of the normalized energy ε and the filter parameter D and for the beryllium foil.

Fig. 21. Normalized double pulse spectrum R_N for beryllium and for lower values of R_N and electron temperature kT_e.

Fig. 22. Filter parameter D for aluminum foil as a function of the electron temperature kT_e and filter thickness d.

Fig. 23. Normalized double pulse spectrum R_N for aluminum.

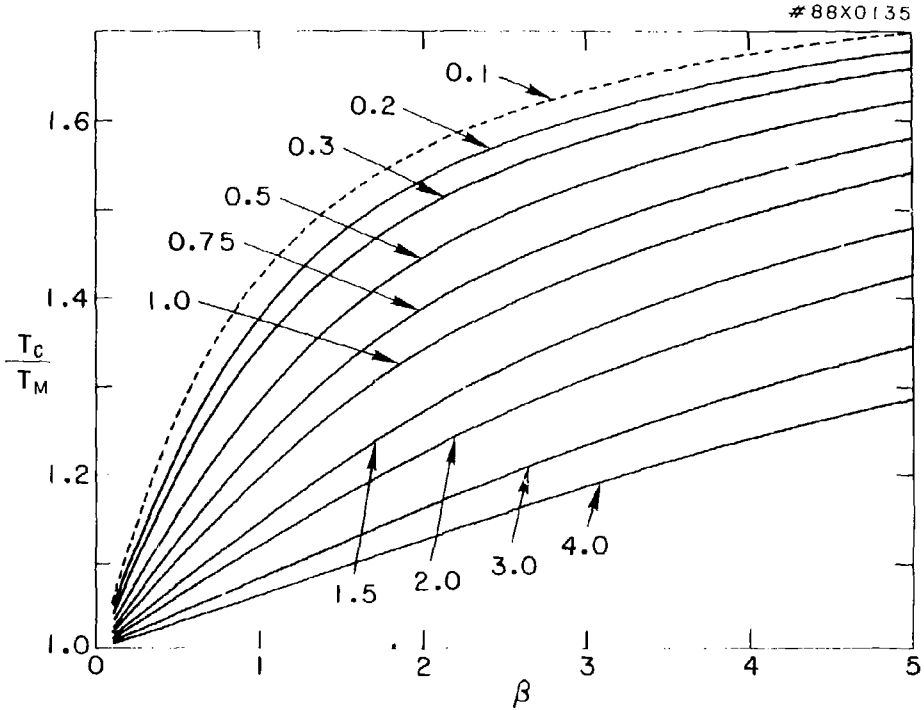
#88X0135
0.1
0.2
0.3
0.5
0.75
1.0
1.5
2.0
3.0
4.0
1.6
1.4
1.2
1.0
$\frac{T_C}{T_M}$
0
1
2
3
4
5
β

Fig. 1

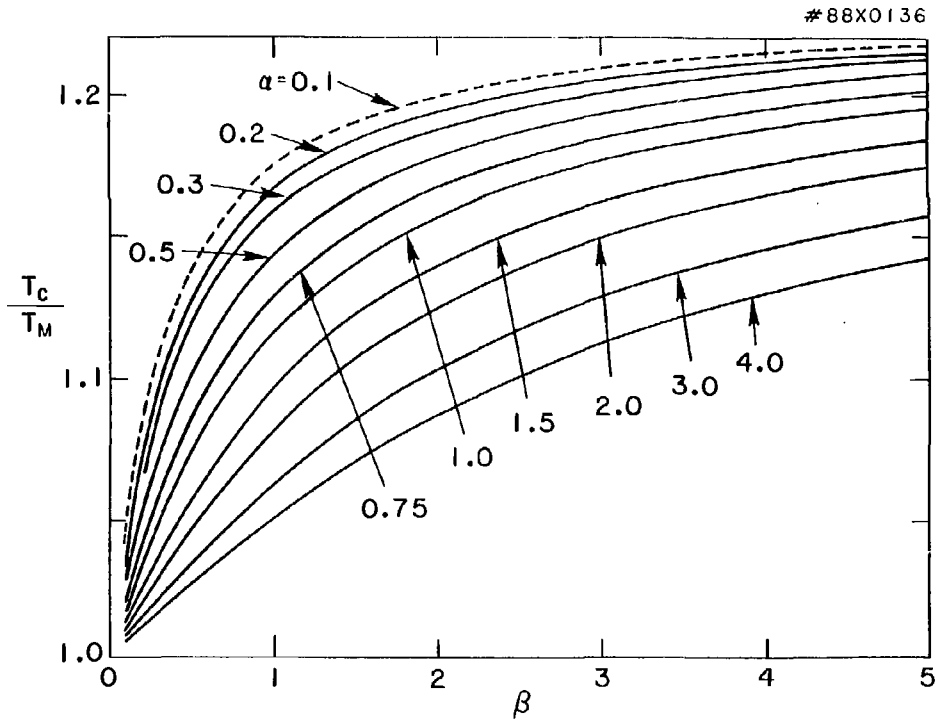
#88X0136
α=0.1
0.2
0.3
0.5
0.75
1.0
1.5
2.0
3.0
4.0
$\frac{T_C}{T_M}$
1.2
1.1
1.0
0
1
2
3
4
5
β

Fig. 2

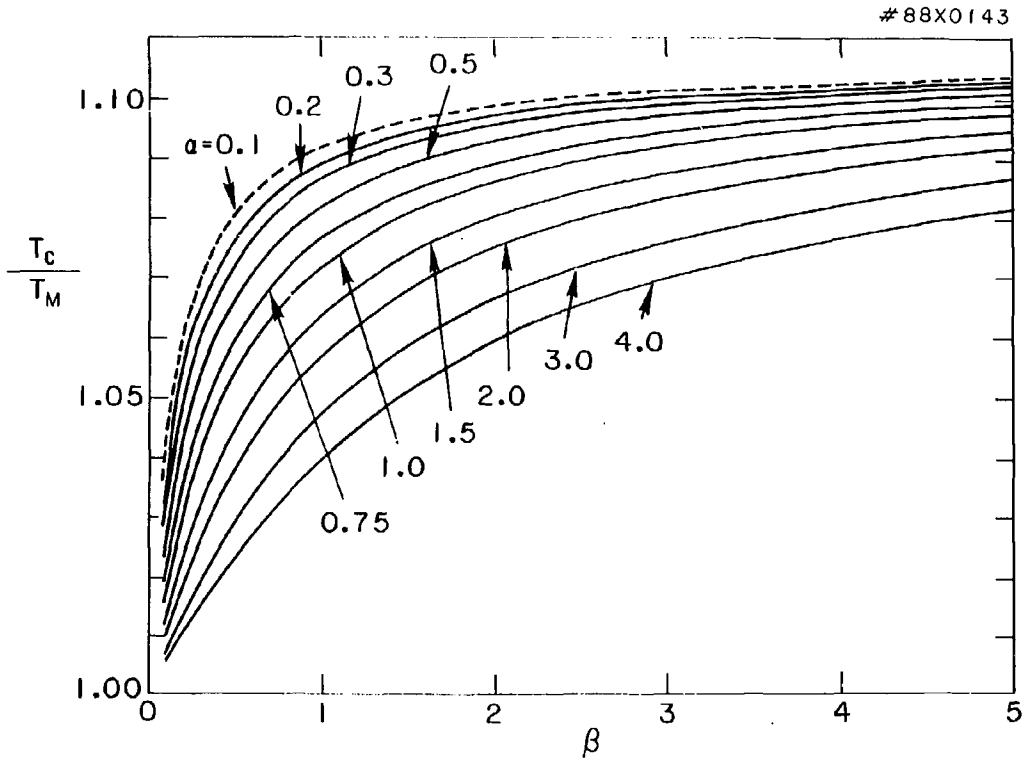
#88X0143
1.10
1.05
1.00
$\frac{T_C}{T_M}$
α=0.1
0.2
0.3
0.5
0.75
1.0
1.5
2.0
3.0
4.0
0
1
2
3
4
5
β

Fig. 3

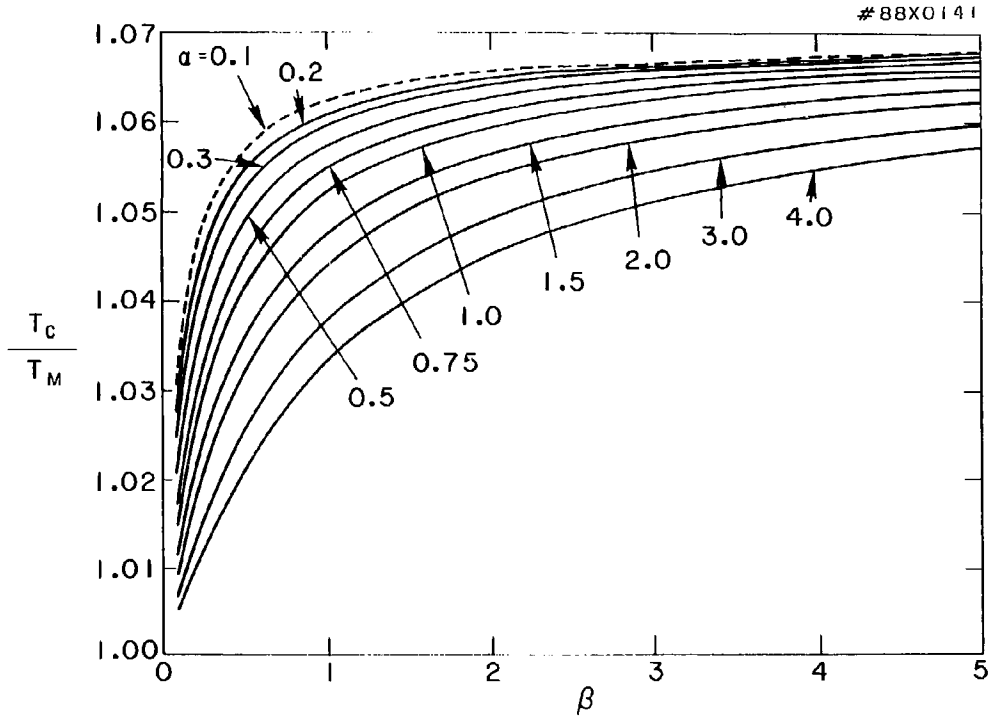
#88X0141
1.07
1.06
1.05
1.04
1.03
1.02
1.01
1.00
$\frac{T_C}{T_M}$
α=0.1
0.2
0.3
0.5
0.75
1.0
1.5
2.0
3.0
4.0
0
1
2
3
4
5
β

Fig. 4

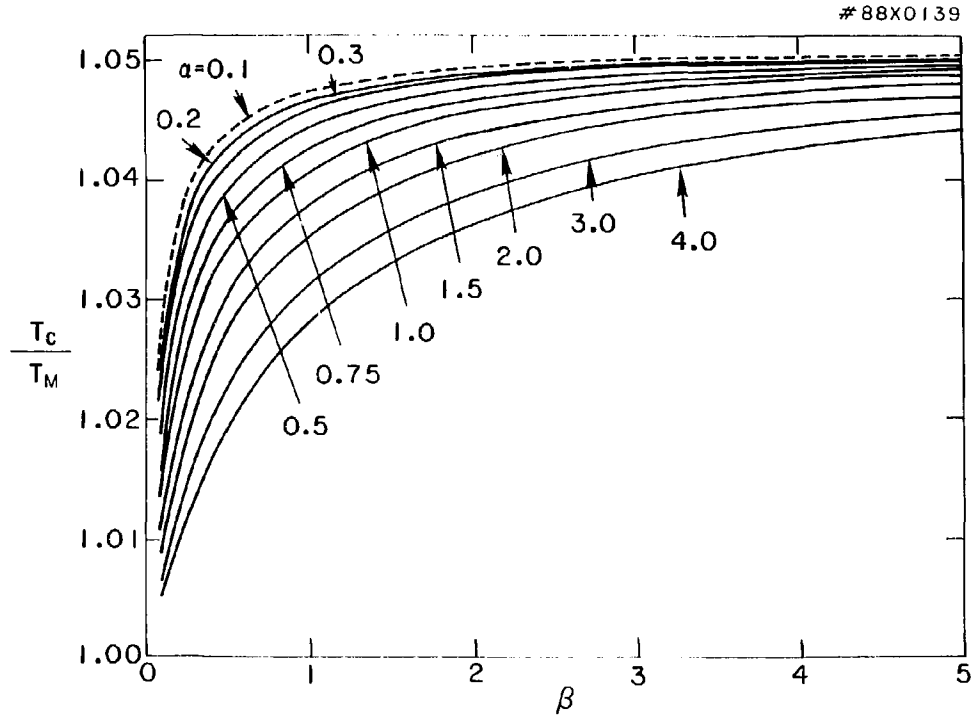
#88X0139
1.05
1.04
1.03
1.02
1.01
1.00
$\frac{T_c}{T_M}$
α=0.1
0.2
0.3
0.5
0.75
1.0
1.5
2.0
3.0
4.0
0
1
2
3
4
5
β

Fig. 5

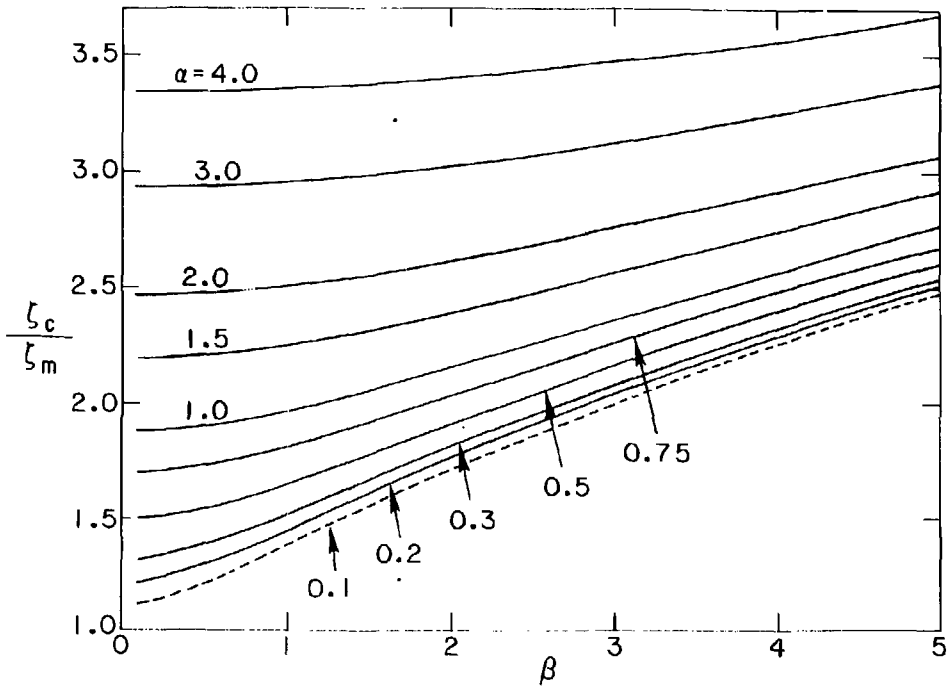
3.5
3.0
2.5
2.0
1.5
1.0
$\frac{\zeta_c}{\zeta_m}$
α = 4.0
3.0
2.0
1.5
1.0
0.75
0.5
0.3
0.2
0.1
0
1
2
3
4
5
β

Fig. 6

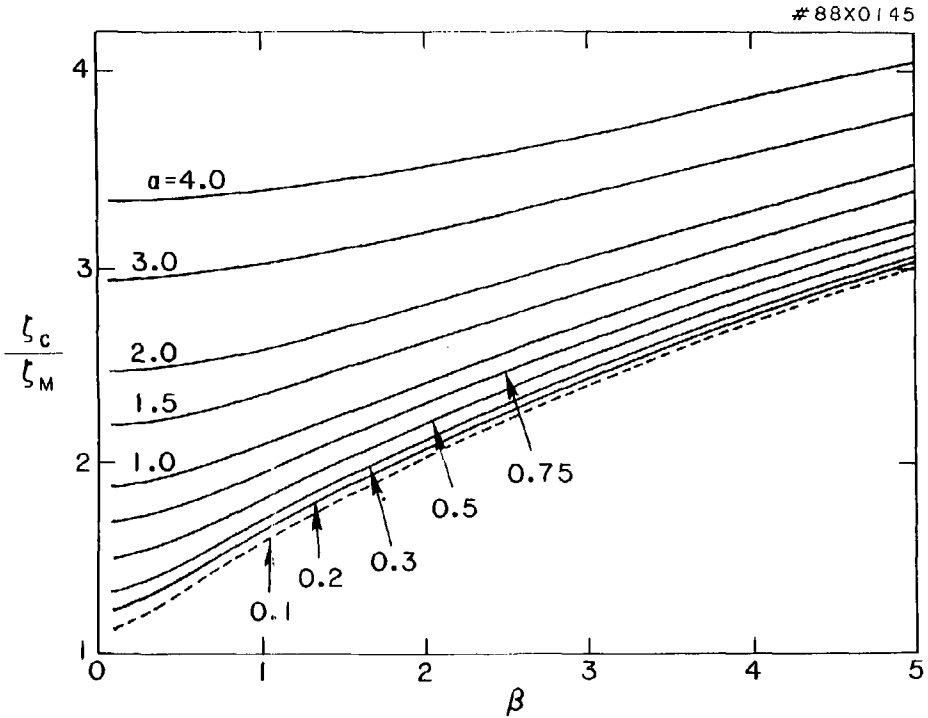
#88X0145
4
3
2
1
0
1
2
3
4
5
$\frac{\zeta_c}{\zeta_M}$
β
a=4.0
3.0
2.0
1.5
1.0
0.75
0.5
0.3
0.2
0.1

Fig. 7

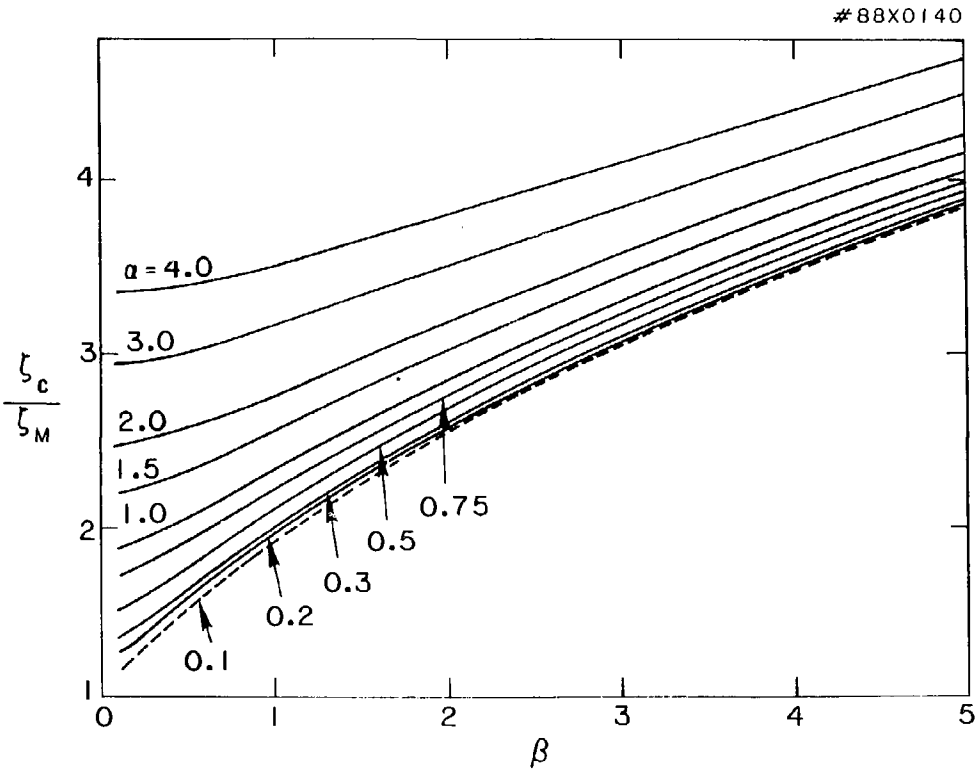
#88X0140
$\frac{\zeta_c}{\zeta_M}$
β
α = 4.0
3.0
2.0
1.5
1.0
0.75
0.5
0.3
0.2
0.1
0
1
2
3
4
5

Fig. 8

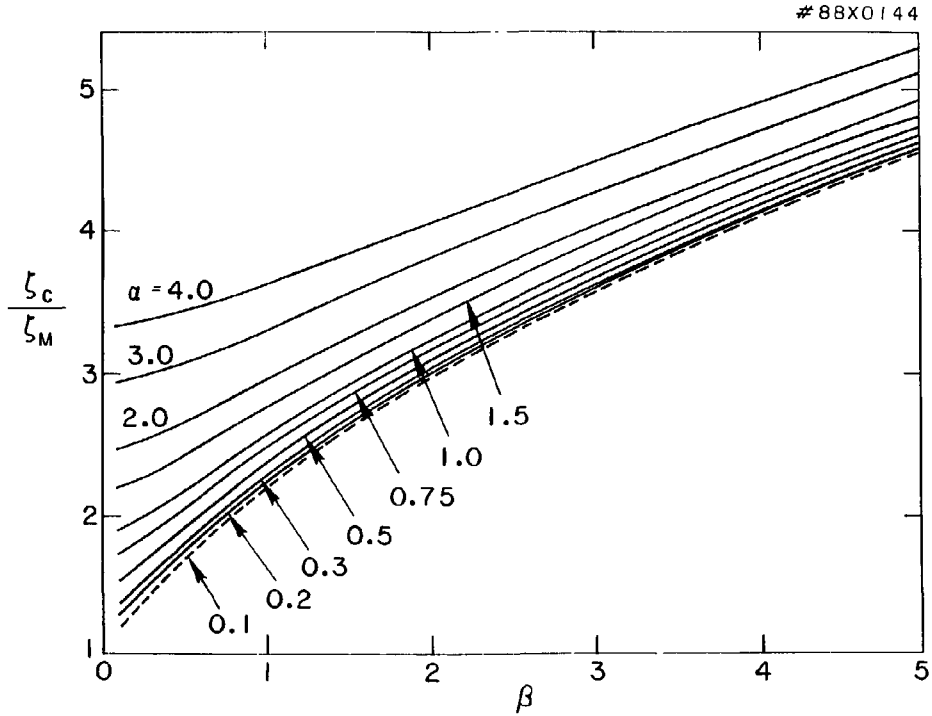
#88X0144
$\frac{\zeta_c}{\zeta_M}$
α = 4.0
3.0
2.0
1.5
1.0
0.75
0.5
0.3
0.2
0.1
β
0
1
2
3
4
5

Fig. 9

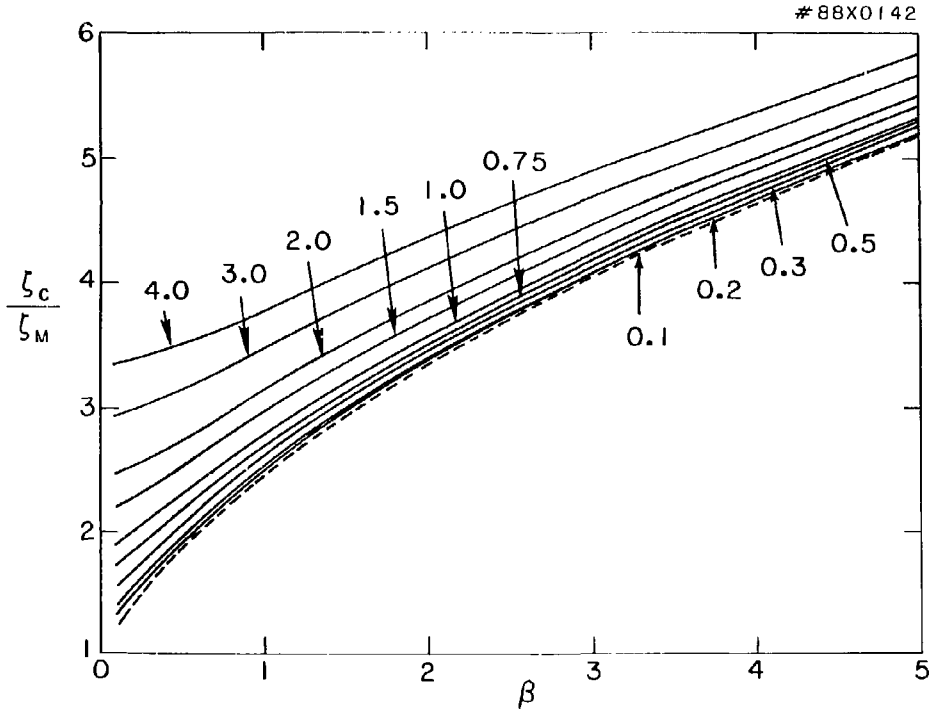
#88X0142
6
5
4
3
2
1
0
1
2
3
4
5
$\frac{\zeta_c}{\zeta_M}$
β
4.0
3.0
2.0
1.5
1.0
0.75
0.5
0.3
0.2
0.1

Fig. 10

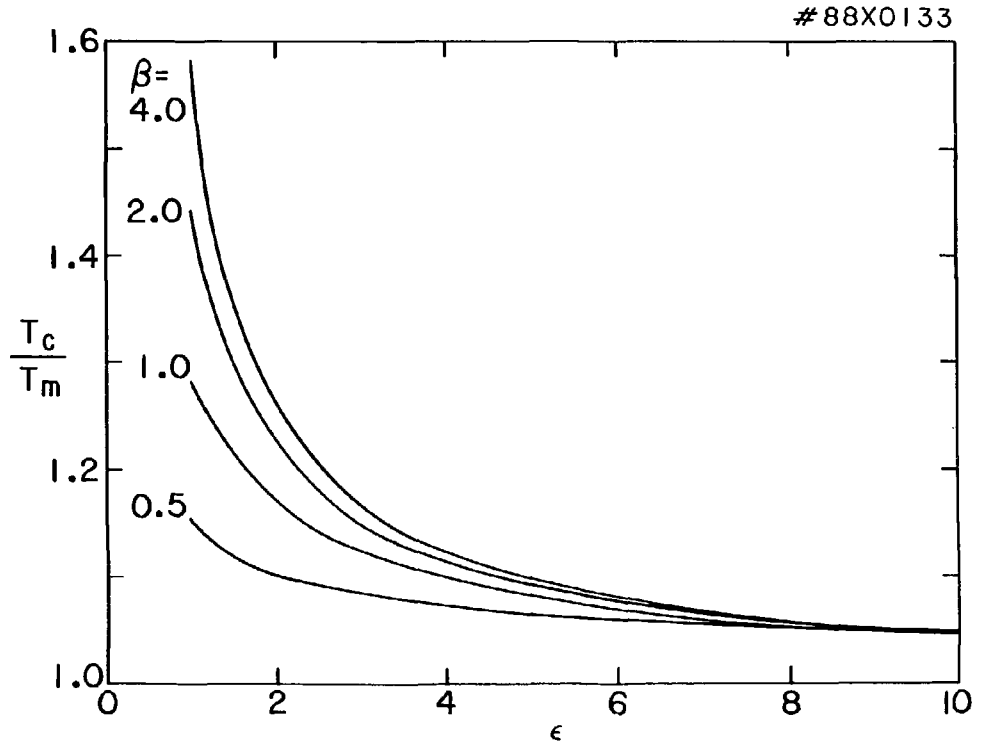

Fig. 11

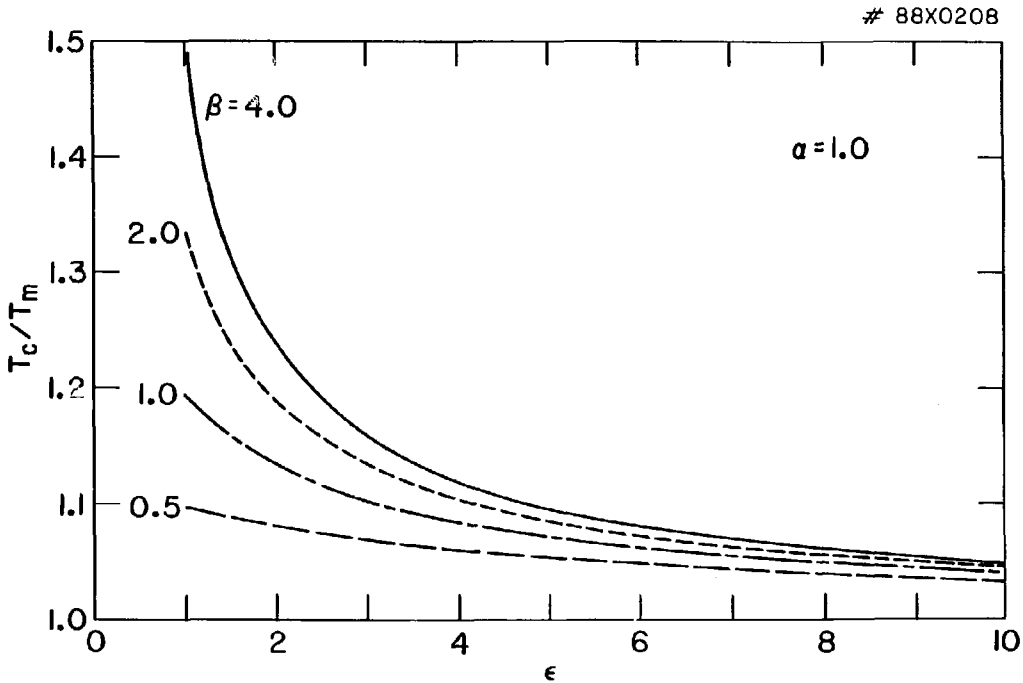
88X0208
1.5
1.4
1.3
1.2
1.1
1.0
T_c/T_m
$\beta = 4.0$
2.0
1.0
0.5
$\alpha = 1.0$
0
2
4
6
8
10
ϵ

Fig. 12

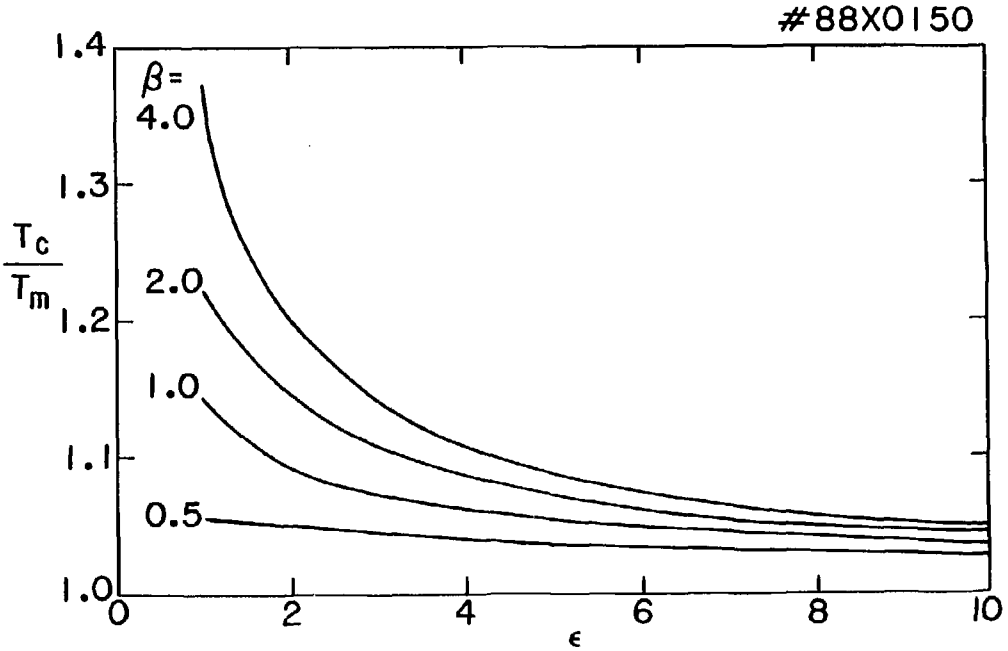

Fig. 13

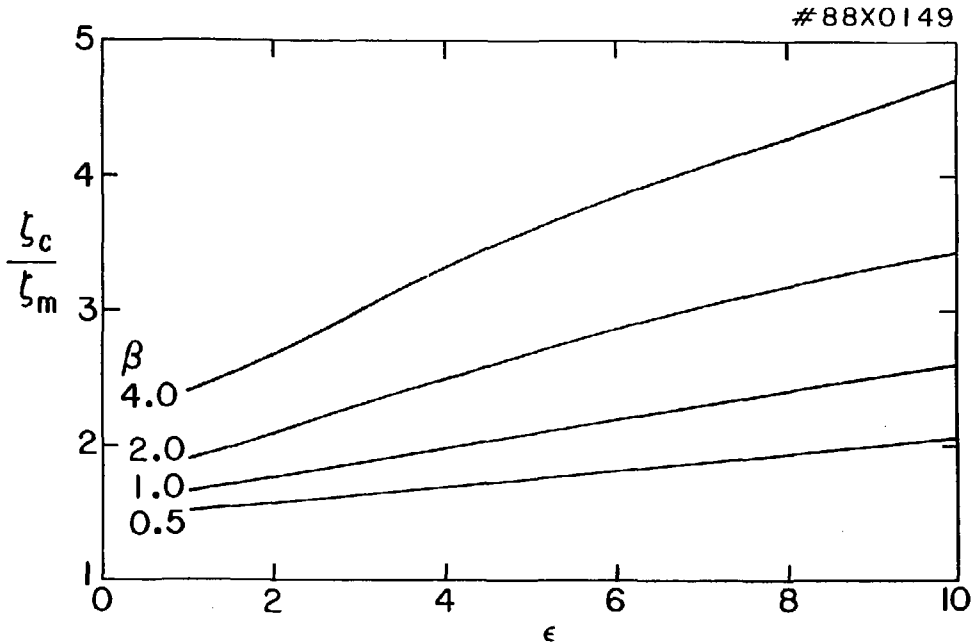
#88X0149
5
4
3
2
1
0
2
4
6
8
10
$\frac{\zeta_c}{\zeta_m}$
ϵ
β
4.0
2.0
1.0
0.5

Fig. 14

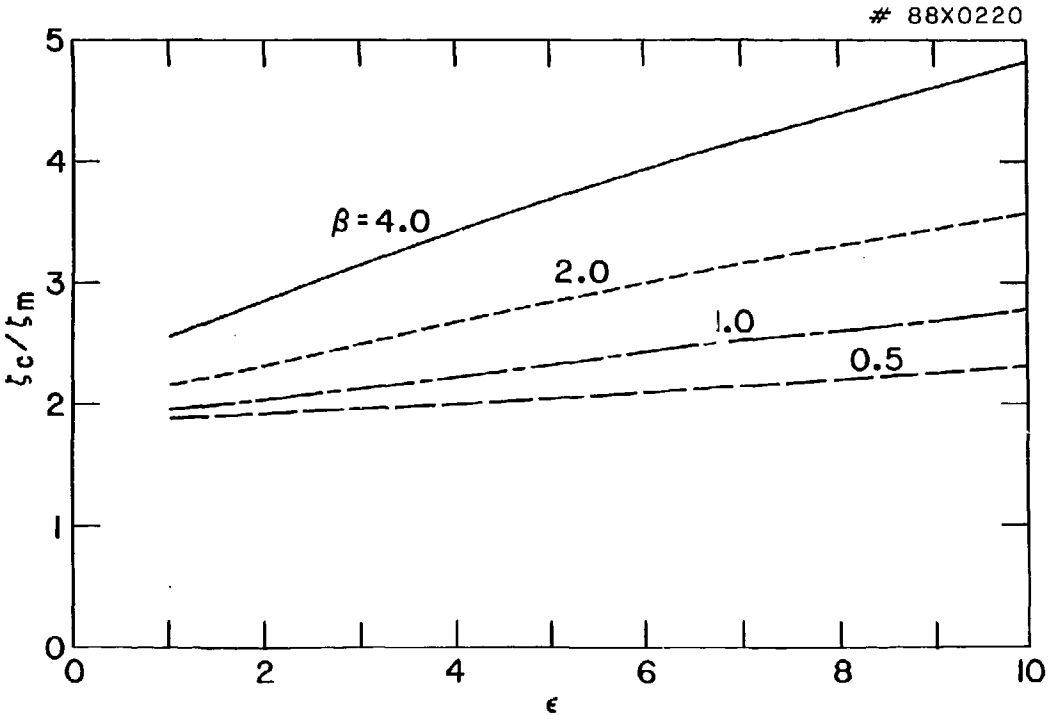

Fig. 15

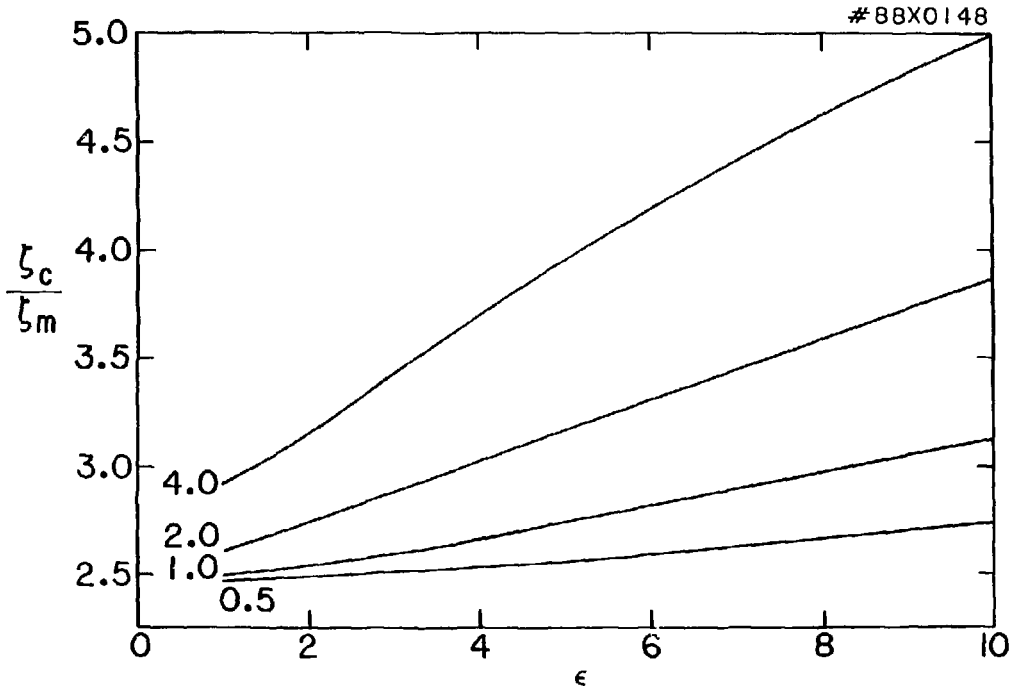
#88X0148
5.0
4.5
4.0
3.5
3.0
2.5
$\frac{\zeta_c}{\zeta_m}$
4.0
2.0
1.0
0.5
0
2
4
6
8
10
ϵ

Fig. 16

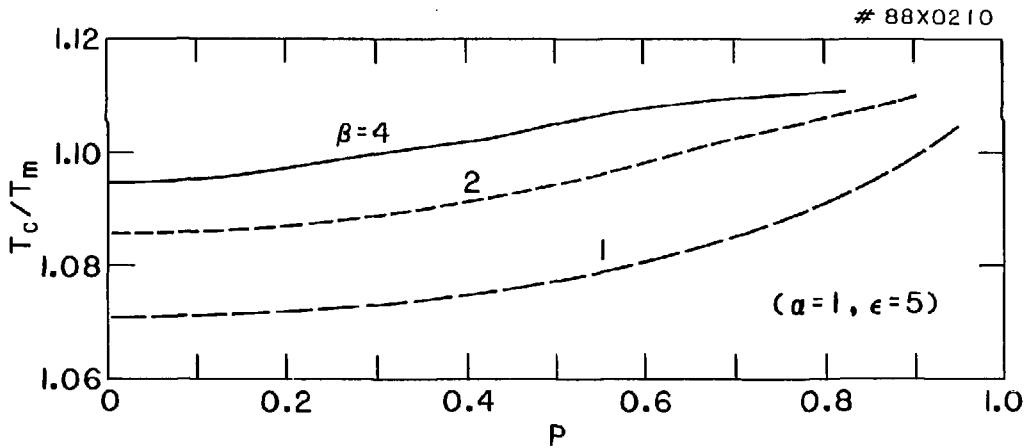
88X0210
1.12
1.10
1.08
1.06
T_c/T_m
$\beta=4$
2
1
$(\alpha=1, \epsilon=5)$
0
0.2
0.4
0.6
0.8
1.0
P

Fig. 17

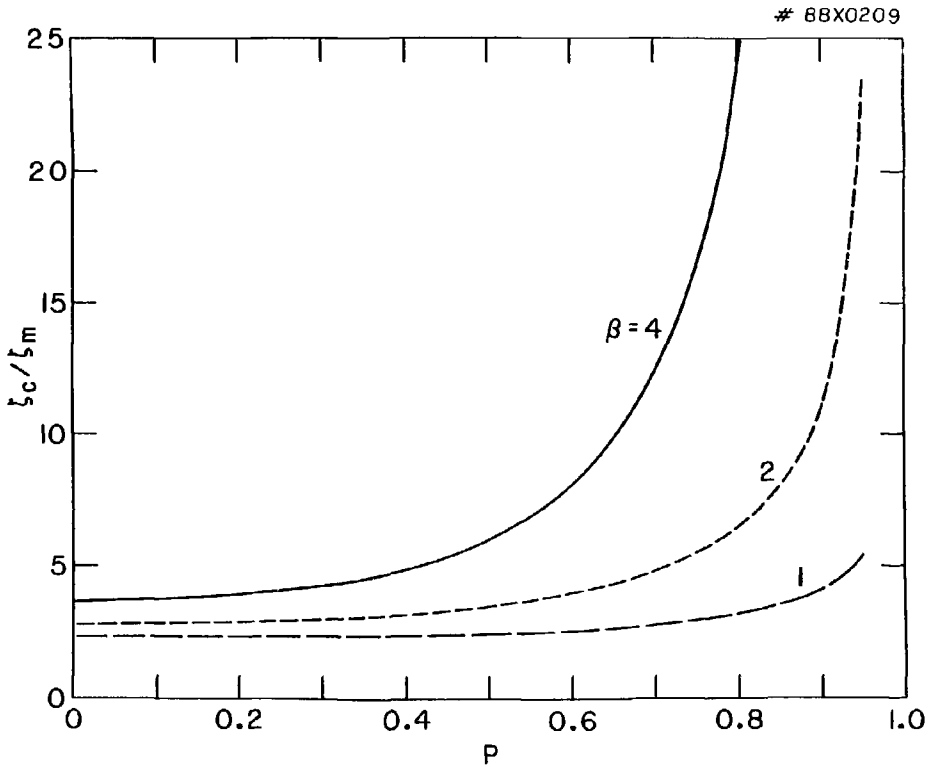

Fig. 18

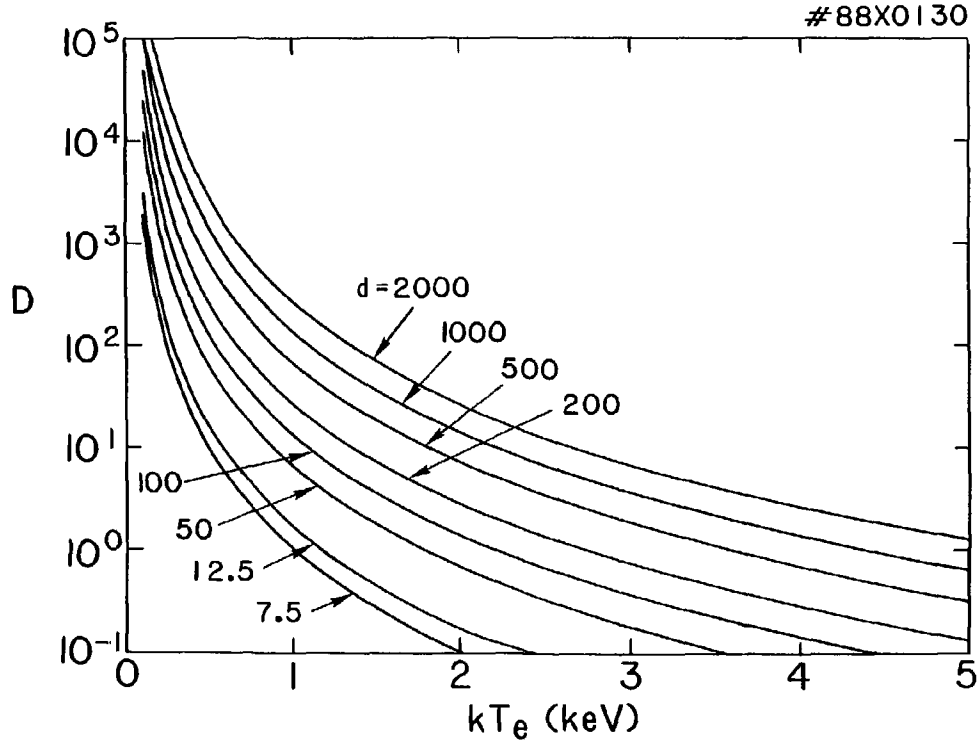
#88X0130
D
10^5
10^4
10^3
10^2
10^1
10^0
10^{-1}
d=2000
1000
500
200
100
50
12.5
7.5
0
1
2
3
4
5
kT_e (keV)

Fig. 19

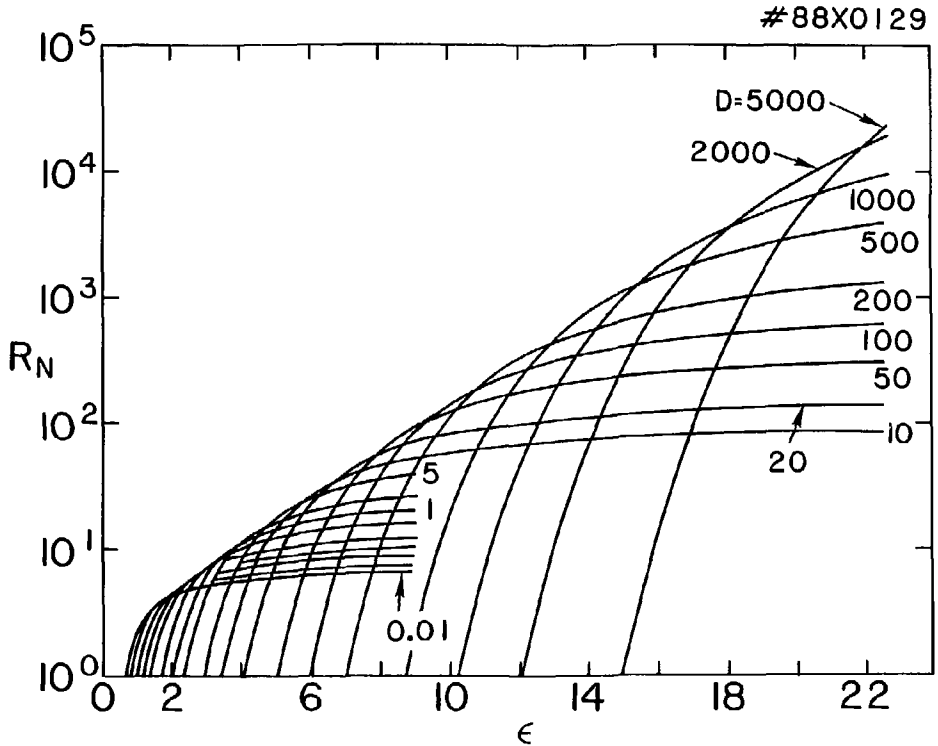
#88X0129
10^5
10^4
10^3
10^2
10^1
10^0
R_N
D=5000
2000
1000
500
200
100
50
10
20
5
1
0.01
0
2
6
10
14
18
22
ϵ

Fig. 30

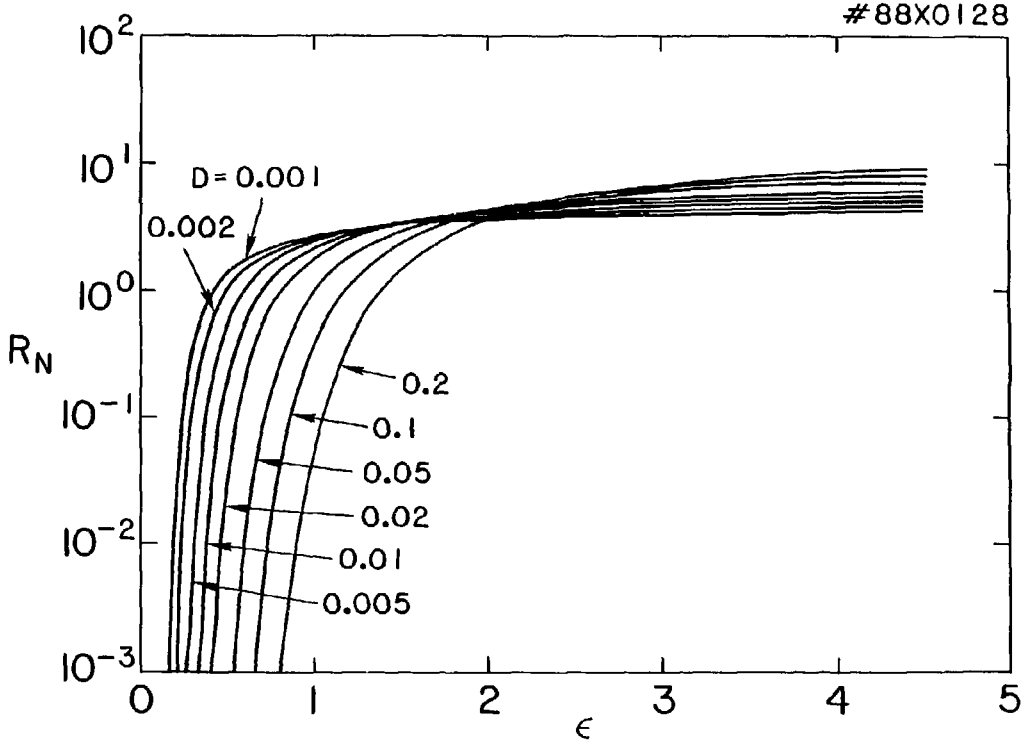
#88X0128
10^2
10^1
10^0
10^{-1}
10^{-2}
10^{-3}
R_N
D = 0.001
0.002
0.2
0.1
0.05
0.02
0.01
0.005
0
1
2
3
4
5
ϵ

Fig. 31

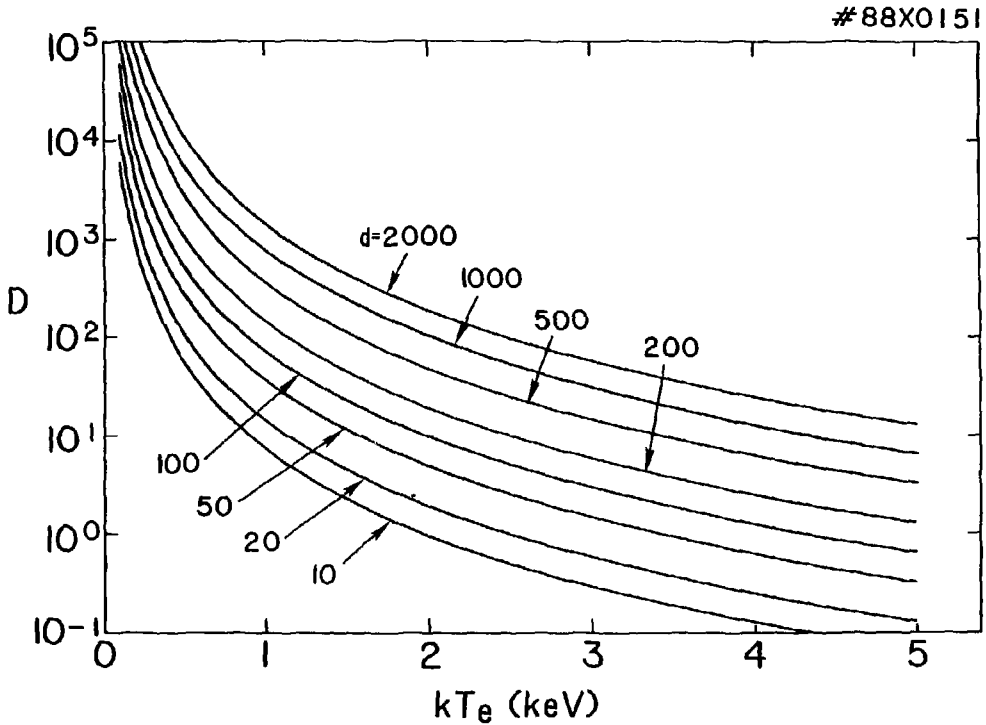
#88X0151
D
10^5
10^4
10^3
10^2
10^1
10^0
10^{-1}
d=2000
1000
500
200
100
50
20
10
0
1
2
3
4
5
kTe (keV)

Fig. 32

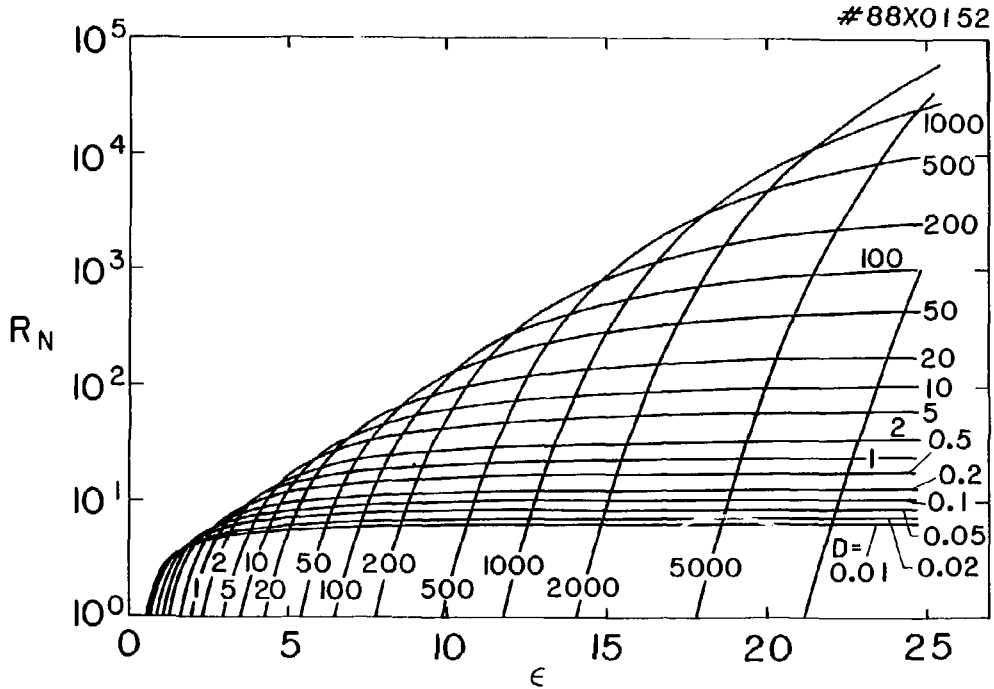
#88X0152
10^5
10^4
10^3
10^2
10^1
10^0
R_N
0
5
10
15
20
25
ϵ
1000
500
200
100
50
20
10
5
2
1
0.5
0.2
0.1
0.05
0.02
D=
0.01
1
2
5
10
20
50
100
200
500
1000
2000
5000

Fig. 23

EXTERNAL DISTRIBUTION IN ADDITION TO UC-20

Dr. Frank J. Paoloni, Univ of Wollongong, AUSTRALIA
Prof. M.H. Brennan, Univ Sydney, AUSTRALIA
Plasma Research Lab., Australian Nat. Univ., AUSTRALIA
Prof. I.R. Jones, Flinders Univ., AUSTRALIA
Prof. F. Cap, Inst Theo Phys, AUSTRIA
Prof. M. Heindler, Institut fur Theoretische Physik, AUSTRIA
M. Goossens, Astronomisch Instituut, BELGIUM
Ecole Royale Militaire, Lab de Phys Plasmas, BELGIUM
Commission-Eurogean, Dg-XII Fusion Prog, BELGIUM
Prof. R. Boucique, Laboratorium voor Natuurkunde, BELGIUM
Dr. P.H. Sakanaka, Instituto Fisica, BRAZIL
Instituto De Pesquisas Espaciasi-INPE, BRAZIL
Documents Office, Atomic Energy of Canada Limited, CANADA
Dr. M.P. Bachynski, MPB Technologies, Inc., CANADA
Dr. H.M. Skarsgard, University of Saskatchewan, CANADA
Dr. H. Barnard, University of British Columbia, CANADA
Prof. J. Teichmann, Univ. of Montreal, CANADA
Prof. S.R. Sreenivasan, University of Calgary, CANADA
Prof. Tudor W. Johnston, INRS-Energie, CANADA
Dr. C.R. James, Univ. of Alberta, CANADA
Dr. Peter Lukac, Komenskeho Univ, CZECHOSLOVAKIA
The Librarian, Culham Laboratory, ENGLAND
The Librarian, Rutherford Appleton Laboratory, ENGLAND
Mrs. S.A. Hutchinson, JET Library, ENGLAND
C. Mouttet, Lab. de Physique des Milieux Ionises, FRANCE
J. Radet, CEN/CADARACHE - Bat 506, FRANCE
Univ. of Ioannina, Library of Physics Dept. GREECE
Dr. Tom Mual, Academy Bibliographic Ser., HONG KONG
Preprint Library, Hungarian Academy of Sciences, HUNGARY
Dr. B. Dasgupta, Saha Inst of Nucl. Phys., INDIA
Dr. P. Kaw, Institute for Plasma Research, INDIA
Dr. Philip Rosenau, Israel Inst. Tech, ISRAEL
Librarian, Int'l Ctr Theo Phys, ITALY
Prof. G. Rostagni, Univ Di Padova, ITALY
Miss Cletia De Palo, Assoc EURATOM-ENEA, ITALY
Biblioteca, Instituto di Fisica del Plasma, ITALY
Dr. H. Yamato, Toshiba Res & Dev, JAPAN
Prof. I. Kawakami, Atomic Energy Res. Institute, JAPAN
Prof. Kyoji Nishikawa, Univ of Hiroshima, JAPAN
Direc. Dept. Large Tokamak Res. JAERI, JAPAN
Prof. Satoshi Itoh, Kyushu University, JAPAN
Research Info Center, Nagoya University, JAPAN
Prof. S. Tanaka, Kyoto University, JAPAN
Library, Kyoto University, JAPAN
Prof. Nobuyuki Inoue, University of Tokyo, JAPAN
S. Mori, JAERI, JAPAN
Librarian, Korea Advanced Energy Res. Institute, KOREA
Prof. D.I. Choi, Adv. Inst Sci & Tech, KOREA
Prof. B.S. Liley, University of Waikato, NEW ZEALAND
Institute of Plasma Physics, PEOPLE'S REPUBLIC OF CHINA
Librarian, Institute of Phys., PEOPLE'S REPUBLIC OF CHINA
Library, Tsing Hua University, PEOPLE'S REPUBLIC OF CHINA
Z. Li, Southwest Inst. Physics, PEOPLE'S REPUBLIC OF CHINA
Prof. J.A.C. Cabral, Inst Superior Tecnico, PORTUGAL
Dr. Octavian Petrus, AL I CUZA University, ROMANIA
Dr. Johan de Villiers, Fusion Studies, AEC, SO AFRICA
Prof. M.A. Hellberg, University of Natal, SO AFRICA
C.I.E.M.A.T., Fusion Div. Library, SPAIN
Dr. Lennart Stenflo, University of UMEA, SWEDEN
Library, Royal Inst Tech, SWEDEN
Prof. Hans Wilhelmson, Chalmers Univ Tech, SWEDEN
Centre Phys des Plasmas, Ecole Polytech Fed, SWITZERLAND
Bibliotheek, Fom-Inst Voor Plasma-Fysica, THE NETHERLANDS
Dr. D.D. Ryutov, Siberian Acad Sci, USSR
Dr. G.A. Eliseev, Kurchatov Institute, USSR
Dr. V.A. Glukhikh, Inst Electrophysical Apparatus, USSR
Dr. V.T. Tolok, Inst. Phys. Tech. USSR
Dr. L.M. Kovrizhnykh, Institute Gen. Physics, USSR
Nuclear Res. Establishment, Julich Ltd., W. GERMANY
Bibliothek, Inst. Fur Plasmaforschung, W. GERMANY
Dr. K. Schindler, Ruhr Universitat Bochum, W. GERMANY
ASDEX Reading Rm, IPP/Max-Planck-Institut fur Plasmaphysik, W. GERMANY
Librarian, Max-Planck Institut, W. GERMANY
Prof. R.K. Janev, Inst Phys, YUGOSLAVIA